Bulletin of Geophysics and Oceanography Vol. 63, n. 1, pp. 99-118; March 2022
DOI 10.4430/bgo00368

Modelling of mineralisation zones formed by oxidation and enrichment processes in porphyry copper deposits using multiple-point geostatistics: the case of Ali-Abad deposit, Iran

H. Mohammadi and O. Asghari

Simulation and Data Processing Laboratory, University College of Engineering, School of Mining Engineering, University of Tehran, Tehran, Iran

(Received: 2 January 2021; accepted: 22 July 2021; published online: 18 January 2022)

ABSTRACT Oxidation and enrichment processes as a secondary phenomenon lead to forming a vertical arrangement of leached, enriched, and hypogene mineralisation zones in porphyry copper deposits. Generating a suitable geological model of these zones can enable a more accurate resource estimation. This research introduces a multiple-point geostatistics simulation (MPS) based workflow to simulate the geological model of such mineralisation zones. The main goal of this workflow is to generate realisations in which: i) the proportions of zones, ii) the vertical arrangement of zones, iii) spatial geometry of the zones, iv) non-stationarity in local proportions are reproduced accurately. Among various MPS algorithms, single normal equation simulation (SNESIM) is used in this study. The proposed workflow includes three main steps: i) constructing an appropriate training image, ii) selecting the best values for SNESIM input parameters, iii) calculating the soft probabilities in order to control the non-stationarity of local proportions. Finally, this workflow was applied to the Ali-Abad porphyry deposit case, and one hundred realisations were generated. The validations have illustrated the acceptance of the realisations in terms of the zones' proportions, the indicator variograms, and vertical mineralogical order of zones, and the local proportion of zones.

Key words: oxidation and enrichment processes, Ali-Abad copper porphyry deposit, multiple-point geostatistics simulation, single normal equation simulation, training image.

1. Introduction

Oxidation and enrichment processes, as a secondary phenomenon, are commonly seen in porphyry copper systems. Sulfide oxidation occurs as an electrochemical process above the water table. If acidic conditions prevail, copper is leached and transferred to the reduced environment just below the water table (Sillitoe, 2005). As a result, the mineralisation vertical profile is divided into different mineralisation zones containing leached, enriched, and primary sulfide zones. Common minerals in the leached zone are goethite, jarosite, hematite, gypsum, alunite and kaolinite. Oxidation and supergene zones often contain oxide minerals including malachite, azurite, chrysocolla, cuprite, chalcocite and covellite. Common minerals in the hypogene zone include pyrite, molybdenite, galena, sphalerite, marcasite, pyrrhotite and copper sulfide (chalcopyrite, bornite, chalcocite and covellite). The leached zone is usually regarded as waste

because it is affected by natural leaching and is poor in terms of copper content. The copper in sulfide ores is extracted by flotation and, in the case of oxide ores, hip heap leaching (Sillitoe, 2005; Berger *et al.*, 2008). Hence, having a more accurate model of these zones, in addition to reducing the risk of over/under grade and tonnage estimation, will lead to appropriate decision-making on how to feed concentrate plants (Dunham and Vann, 2007). It is clear that a model of subsurface phenomena is accurate when its geological knowledge and concepts are considered in the modelling. The intensity of oxidation and enrichment processes varies based on different controllers at different locations of deposits (Sillitoe, 2005). Therefore, the vertical thickness of zones has a type of non-stationarity that must be taken into account in the process of modelling (Boucher *et al.*, 2006; Emery, 2007; Talebi *et al.*, 2013).

In mining operations, having a model of geological zones that control the mineralisation grade is necessary for making accurate resource estimation and suitable future mine planning. In recent decades, researchers have considered stochastic tools for subsurface geological modelling (Talebi *et al.*, 2013, 2014, 2015; Tehrani *et al.*, 2013; Rezaee *et al.*, 2014; Hosseini and Asghari, 2016; Talesh Hosseini *et al.*, 2020). Stochastic geostatistical techniques provide different realisations of the phenomena under study. While having the same statistical properties, each of these realisations presents a different scenario for the occurrence of a phenomenon (Talebi *et al.*, 2013; Rezaee *et al.*, 2014; Talesh Hosseini *et al.*, 2020). In this context, two-point geostatistical simulation methods use variograms. Because a variogram takes two points at a time to measure spatial relationships, it is not an effective tool for simulating complex geological settings (Rezaee *et al.*, 2014).

Given the need for a tool to investigate multiple-point relationships, Guardiano and Srivastava (1993) introduced a multiple-point geostatistics simulation (MPS) using the so-called technique of training image (TI). A TI is a conceptual tool that exemplifies the spatial structure to be reproduced (Tahmasebi, 2018). Following the introduction of MPS, researchers proposed several MPS implementation algorithms. Mariethoz *et al.* (2015) divided these algorithms into two general categories. The first is based on a sequential indicator simulation (SIS) that obtains all required conditional probabilities through scanning the TI. The single normal equation simulation [SNESIM: Strebelle (2002)] and its memory-efficient version [IMPALA: Straubhaar *et al.* (2013)], lie in this category. The second category includes MPS algorithms that are based on the computation of distances between data events; examples are direct sampling (DS) (Mariethoz *et al.*, 2010) and its bunch-based version (Rezaee *et al.*, 2013). Generally, MPS is designed to consider information related to constraints (Mariethoz and Caers, 2014). Sufficient knowledge of subsurface geological phenomena is usually available. This knowledge can be applied, in the form of a TI, to MPS results. In this context, Rezaee *et al.* (2014) presented a model for the dykes of the Sungun porphyry system, in which the dykes' continuity was considered as part of geological knowledge. Creating a TI in which the dykes' continuity is visible, they performed satisfactory realisations through the SNESIM algorithm. TI is an important input parameter of MPS methods. Therefore, any mistake in these assumptions will lead to unrealistic results (Pyrcz *et al.*, 2008; Mariethoz and Caers, 2014; Abdollahifard *et al.*, 2019).

In MPS algorithms, a random function distribution is modelled by a TI that is assumed stationary (Strebelle, 2002); however, real cases might display non-stationarity in the proportion of their zones (Emery, 2007; Talebi *et al.*, 2013). Arpat and Caers (2007) proposed that a variable consists of a trend and a residual, and the former can be applied to the model by using soft probabilities. By performing a calibration operation between soft and hard data, it is possible to convert soft data into soft probabilities of zones. While hard data sets, such as drillhole data, present direct information about the phenomenon under study, soft data sets refer to

low-resolution data sets that are indirectly related to the phenomenon in question. An example might include the calibration between seismic data (soft data) and well data (hard data) through multinomial logistic regression in order to generate soft probabilities of a zone's occurrence in a gas field (Rezaee and Marcotte, 2017). In other researches, e.g. Plurigaussian simulation (PGS) studies, the vertical proportion matrix (VPM), calculated through drillhole data analysis, has been used as soft probabilities (Beucher-Darricau et al., 2006; Emery, 2007; Talebi et al., 2013).

2. Methodology

The main goal of this paper is to propose an MPS-based approach to simulate oxidation and enrichment zones in porphyry copper deposits, so that the mineralogical order of the zones and their non-stationarity approximate the real situation in the final model. Several implementation MPS algorithms such as SNESIM (Strebelle, 2002) and IMPALA (Straubhaar *et al.*, 2013), SIMPAT (Arpat and Caers, 2007), FILTERSIM (Zhang *et al.*, 2006), DS (Mariethoz *et al.*, 2010) and its bunch-pasting version (Rezaee *et al.*, 2013), have been introduced. Among these algorithms, the SNESIM algorithm was chosen to use in this study. The important reason for this is the successful straightforward implementation and low computational cost of this algorithm in the open source Stanford geostatistical modelling software package known as SGeMS (Remy *et al.*, 2009).

The workflow steps followed in this study include: first, a TI is constructed on some geological and statistical criteria and evaluated based on measuring the consistency between TI's multiple point patterns and the drillhole's multiple point patterns. Next, through a trial and error approach, the best values are selected for the SNESIM input parameters. Addressing the non-stationarity of local proportions is the last step of the proposed methodology.

In the following, first the SNESIM algorithm is presented in summary form, then the workflow steps are presented in detail.

2.1. SNESIM algorithm

Based on the idea by Guardiano and Srivastava (1993), Strebelle (2002) developed the SNESIM algorithm. It is an efficient pixel-based SIS algorithm that obtains all required conditional probabilities through scanning a TI. Since it is a pixel-based simulation method, it is flexible at respecting the hard conditioning data. The SNESIM procedure for simulating categorical variable Z is as follows (Strebelle, 2002; Mariethoz and Caers, 2014; Hansen *et al.*, 2016):

1. assign each conditioning point to the simulation grid nodes;
2. define a fixed n-point search template;
3. scan the TI by defined search template and save each found pattern with its replicate in a search tree;
4. define a random path for simulation grid nodes, for each visited node x in this path:

4.1. find the neighbourhood of x considering the defined search template T, denoted as N_x;

4.2. calculate the conditional probability distribution of $Z(x)$ conditional to N_x considering search tree patterns;

4.3. sample a value from obtained conditional probabilities and place it in x node;

4.4. assign simulated node x to hard conditioning data.

2.2. TI construction

Since all assumptions about the model under consideration are explicitly stated in the TI, it is assumed as an important algorithm building block of each MPS algorithm (Mariethoz and Caers, 2014). One of the challenges of applying MPS methods to 3D simulations consists in selecting a suitable 3D TI. Previous studies have attempted to meet this challenge by means of various approaches, the most important of which are: i) selecting the geological model of a previously mined-out area as a TI (Rezaee *et al.*, 2013; Osterholt and Dimitrakopoulos, 2018); ii) introducing an approach for using 2D TI, such as maps and geological sections, to develop 3D simulations (Comunian *et al.*, 2012); and iii) the available knowledge of the phenomenon under study is used to generate a number of TIs through object-based methods such as TI-selector (Maharaja, 2008) and FLUVSIM (Pyrcz *et al.*, 2008), then, the best TI is selected based on the maximum compatibility between TI's patterns and the patterns of drillhole data (Boisvert *et al.*, 2008; Pyrcz *et al.*, 2008; Pérez *et al.*, 2014).

In order to construct a representative TI of the leached, enrichment and hypogene zones, three important criteria are considered: i) global proportions of zones, ii) vertical order of zones, and iii) the spatial geometry of zones. Finally, the constructed TI is evaluated by means of measuring the consistency between TI's patterns and the patterns of drillhole data.

2.2.1. Global proportions

One of the important goals of geostatistical simulation is to reproduce the target proportion of zones in the realisations. It should be noted that the target ratios are those obtained from the analysis of drillhole data. Strebelle (2002) introduced a servosystem correction [$\lambda \in (0,1)$] for the SNESIM program. Even if λ becomes closer to value 1, the proportion of the simulated zones will be closer to the targets, but the risk of losing desired geological patterns increases. Considering the trade-off between achieving target proportions and patterns reproduction, Liu (2006) recommended selecting a TI whose global proportions are close to those of the targets. In this case, it is possible to both generate realisations that have proportions equal to those of the targets and reduce the risk of losing TI patterns because of the increase in λ. Therefore, one of the criteria to be fulfilled in constructing a TI is that the proportions of TI zones must be similar to those of the target.

2.2.2. Vertical order

One of the main goals of this research is to determine the mineralogical order of the zones in the realisations. So, there is a need for an instrument such as transition probability matrix to quantify the concept of vertical order of the mineralisation zones. The transition probability from zone K_1 to zone K_2 for lag h is equal to the proportion of the number of two point spatial patterns, given that $Z(u)$ is in category k_1 and that $Z(u + h)$ is in category k_2:

$$f(k_i, k_j, h) = \text{Prob}\left(Z(u) \in k_i \,\&\, Z(u+h) \in k_j\right), k_i, k_j = 1, 2, \ldots, K. \quad (1)$$

The output of this tool is a $K \times K$ matrix that determines the transition probability between pairs of zones as the proportion of all occurrence transitions (Pyrcz *et al.*, 2008). For example, the probability of transition from lithofacies k_1 to lithofacies k_2 for lag h is calculated by dividing the

number of the replicate of this transition to the number of the replicate of transitions between all *K* lithofacies:

$$\text{Prob}\,(Z(u) \in k_1\ \&\ Z(u+h) \in k_2) = \frac{\text{count}\,(Z(u) \in k_1\ \&\ Z(u+h) \in k_2)}{\sum_{i,j=1}^{K} \text{count}\left(Z(u) \in k_i\ \&\ Z(u+h) \in k_j\right)}. \quad (2)$$

Therefore, the second criterion in constructing a representative TI is that the transition probability matrix of the TI for lag *h* (*x, y, z*) = (0, 0, +1) must be the same as the transition probability matrix of drillhole data. It should be noted that *h* (*x, y, z*) = (0, 0, +1) means the upward transition between two vertical conjunct locations. With respect to lag *h* (*x, y, z*) = (0, 0, +1) some transition probabilities should be zero, i.e. they are geologically impossible (Fig. 1).

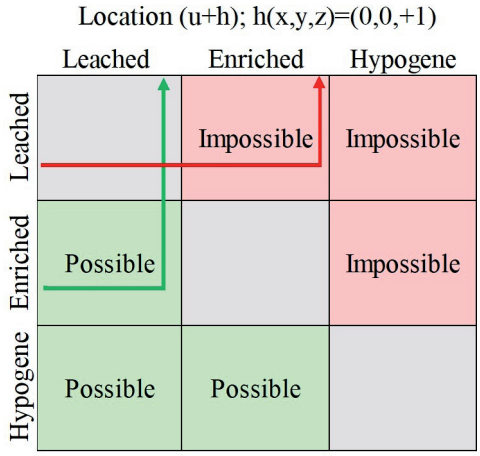

Fig. 1 - Transition probability matrix for lag *h* (*x, y, z*) = (0, 0, +1) of leached, enriched and hypogene zones. Grey elements: transition between locations, which are in same zone. They are not involved in the calculations. Green elements: they are geologically possible, i.e. transition from enriched zone to leached zone, which illustrated by green arrows. Red elements: they are geologically impossible, i.e. transition from leached zone to zone enriched illustrated by red arrows.

2.2.3. Spatial geometry

In addition to the two previous criteria, there is a need for a concept whereby the spatial geometry of zones becomes realistic. King (1899) observed that groundwater depth is linked to topography. In other words, the water table depth is a function of surface topography (Condon and Maxwell, 2015). Also, the enrichment process occurs just under the water table (Sillitoe, 2005). Therefore, the top surface of the enrichment zone can be a function of surface topography. Thus, by imposing the topography of the area under study on the TI constructed based on the two previous criteria, the spatial geometric variations of contact zones can be made more realistic. It should be noted that, owing to various controllers that influence oxidation and enrichment processes, such a correlation between Z_1 (surface topography) and Z_2 (top surface of enrichment zone) may not be observed in all porphyry copper deposits. In such cases, the indicator variogram of each zone in drillhole data could be used as a criterion for controlling the spatial geometric variation of the zones in the TI.

2.2.4. TI evaluation

MPS-based algorithms use TIs with 3D multi-point patterns. Hence, to avoid any mistakes in the simulation results, it is important to check whether the constructed TI is representative of the 3D patterns observed in drillhole data. In this regard, Boisvert al. (2008) presented an approach for comparing multi-point patterns that are defined by a fixed 1D vertical template between the TI and drillhole data. Because MPS algorithms use 3D TI patterns to simulate subsurface phenomena, it is better to use a 3D template for such a comparison. Pyrcz *et al.* (2008) proposed an MPSTAT program that uses a 3D fixed template to compare multi-point patterns between data and a TI. When the number of template nodes (*n*) or the number of facies (*k*) is too high, such programs are not applicable due to their high computational cost. Perez *et al.* (2014) introduced a tool called Absolute Compatibility that performs a comparison between drillhole data and TI 3D patterns, and it does not involve any of the abovementioned problems. Accordingly, all data are first assigned to a Cartesian grid. Then, each node (*i*) of this grid is selected as the central node in a random path. A spherical search is performed around the central node until *n*-informed nodes are found. The *n*-point patterns known as conditional data events (CD_i) will be obtained through this search. The TI is then scanned based on the pattern found in the data. The first time a CD_i-matched pattern occurs in the TI, the *Yi* indicator is given a value of 1, but if the entire TI is scanned and no CD_i-matched pattern is found, this indicator is given a value of 0. Eventually, using Eq. 3, where *I* is the total number of searched patterns, we can calculate absolute compatibility as absolute CD_i-matched pattern proportions (MP). The greater the consistency between drillhole data patterns and TI patterns is, the closer the value will be to 1:

$$\text{Absolute comptability} = \frac{\sum_{i=1}^{1} Y_i}{I} \in (0,1). \quad (3)$$

2.3. SNESIM input parameters

Although TI is the most important input of SNESIM, the reproduction of target statistics and desirable geological patterns are also dependent on other advanced SNESIM parameters. Accordingly, the best definitions for these parameters include the servo-system correction factor (λ), the search ellipsoid geometry, the minimum replication of patterns in TI, and the number of multi-grids (Tran, 1994). According to Liu (2006), minimum replication of patterns and the number of multi-grids can be set to 12 and 4, respectively.

The search ellipsoid geometry is the basis for calculating conditional probabilities in SNESIM, hence its notable impact on the reproduction of TI desirable patterns. In addition, the servo-system correction factor helps reproduce target proportions, but its increase may have a detrimental effect on the reproduction of TI patterns. The most suitable definition of search ellipsoid geometry leads to the best reproduction of TI patterns in the realisations, and selecting the best value for the servo-system correction factor results in both the best target proportions and the reproduction of TI patterns in simulation results. It should be noted that target proportions are obtained from drilling data. Furthermore, to investigate the reproduction of desirable patterns, we can choose the transition probability matrix of drillhole data as a target. While other parameters have a constant value, different values could be assigned to the desired parameter. In each case, a realisation is generated by the SNESIM algorithm and, then, evaluated based on the degree to which the desired targets have been met.

Each of the resulting targets is a type of probability distribution function. Therefore, there is a need for a tool capable of performing a convenient comparison between two probability distribution functions. In this regard, the Jensen-Shannon divergence (JSD) is an effective norm. It is based on the Kullback-Liber divergence, and it has significant advantages, including symmetricity and finiteness, which is computed as:

$$\mathrm{JSD}(p\|q) = \frac{1}{2}K(p\|q) + \frac{1}{2}K(p\|m) \quad \text{where } m = \frac{p+q}{2} \tag{4}$$

K is the Kullback-Liber divergence, which is defined as:

$$K(p\|q) = \sum_{j=1}^{J} \log\frac{p_i}{m_j} p_j \tag{5}$$

If one uses the base 2 logarithm, the JSD divergence is obtained in (0, 1). Therefore, in this study, we used JSD and calculated it using logarithm base 2. If the value of this divergence is zero, the two countable probability distributions will be the same; alternatively, as this value becomes closer to one, the difference between the two probability distribution functions increases.

2.4. Non-stationarity of local proportions

Oxidation and enrichment processes occur with different intensities at different locations, consequently, mineralisation zones display non-stationarity in local proportions. In terms of achieving realisations with low uncertainty, this non-stationarity must be reproduced in the realisations. In MPS algorithms, a random function distribution is modelled by a TI that is assumed to be stationary (Strebelle, 2002); however, real cases might display non-stationarity in the proportion of their zones. Arpat and Caers (2007) proposed that a variable consists of a trend and a residual, and the former can be applied to the model by using soft probabilities.

By performing a calibration operation between soft and hard data, it is possible to convert soft data into soft probabilities of zones occurrences. Soft data are low-resolution data sets that are indirectly related to the phenomenon in question. An example might include calibration between seismic data (soft data) and well data (hard data) through multinomial logistic regression in order to generate soft probabilities of a zone's occurrence in a gas field (Rezaee and Marcotte, 2017). In some studies, especially Plurigaussian simulation applications (PGSs), the VPM (Beucher-Darricau *et al.*, 2006) is computed through drillhole data analysis and the results are used as soft probabilities in the simulation (Emery, 2007; Talebi *et al.*, 2013). Vertical proportion curves (VPC) are tools for determining the proportion of different zones as a function of depth (Matheron *et al.*, 1987). In real cases, due to lateral variations, it is better to use a matrix of VPC, instead of a fixed VPC, for the entire area. VPM is a 3D grid of each pixel, which contains the probability of each zones occurrence (Ravenne *et al.*, 2002).

In this study, in order to address non-stationarity of local proportions, it is proposed to calculate the VPM and use it as soft probabilities in SNESIM. In calculating VPCs, the reference level highly affects the results and any mistake in its selection could result in losing the continuity of zones in the realisations (Armstrong *et al.*, 2011). According to the explanations given in the previous

section, regarding the relationship between surface topography and the enrichment process, surface topography should be chosen as the reference level to calculate VPCs. In SNESIM, this non-stationarity is resolved through a probability aggregation model. During the sequential simulation mode, the conditional probability of hard data $P(A|B)$ is calculated at each location based on the TI. In a probability aggregation model, $P(A|B)$ is combined with the co-located soft probability $P(A|C)$ to calculate $P(A|B.C)$, which is conditioned to both hard and soft data (Liu, 2006). In other words, soft probabilities are used to control non-stationarity in the simulation results.

3. The case of Ali-Abad porphyry copper deposit

The Ali-Abad porphyry copper deposit is located 60 km SW of Yazd, central Iran (Fig. 2a). The host rock in this deposit consists of quartz monzodiorite, granodiorite and granite, which have undergone intense fracturing and healing that led to the formation of quartz-sulfide veinlets (Zarasvandi *et al.*, 2005). The simple geological map of Ali-Abad deposit is shown in Fig. 2b.

Ali-Abad deposit was sampled by core drilling at 67 locations (Fig. 3) with an average spacing of 100 m. The drillhole data set, which is available for this study includes 2,108 sample points (2-m composites), which are logged geologically in addition to the assays for the copper. According to primary exploratory data analysis (Fig. 4), Ali-Abad is a low-grade porphyry copper deposit. Although the oxidation and enrichment processes have a limited impact on the deposit, they still strongly control the grade of ore copper content (Fig. 4).

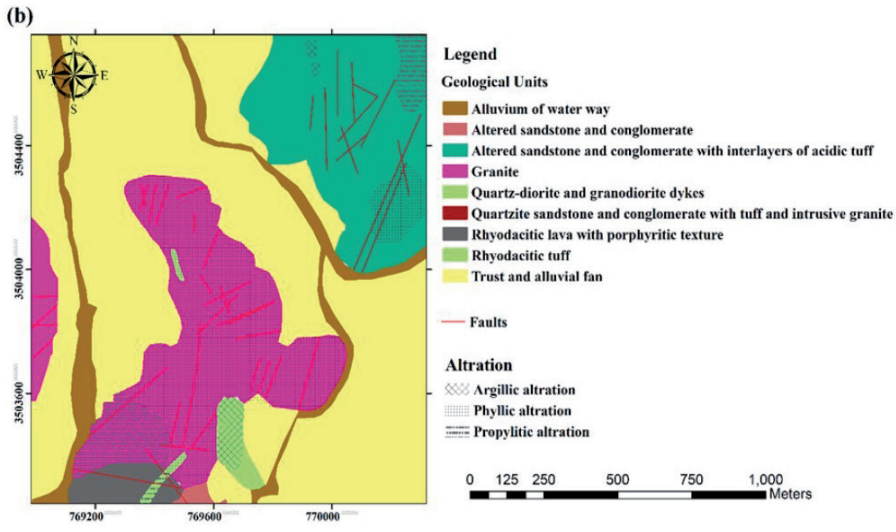

Fig. 2 - Ali-Abad copper deposit: a) relative location of Ali-Abad deposit in Iran; b) simplified geological map of Ali-Abad copper deposit (Zarasvandi *et al.*, 2005).

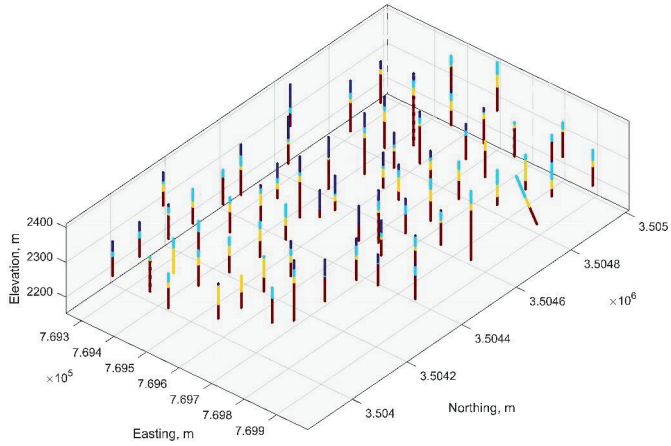

Fig. 3 - 3D view of the whole data set. Dark blue colour refers to alluvium zone, light blue to leached, yellow to enriched, and red to primary sulfide zone.

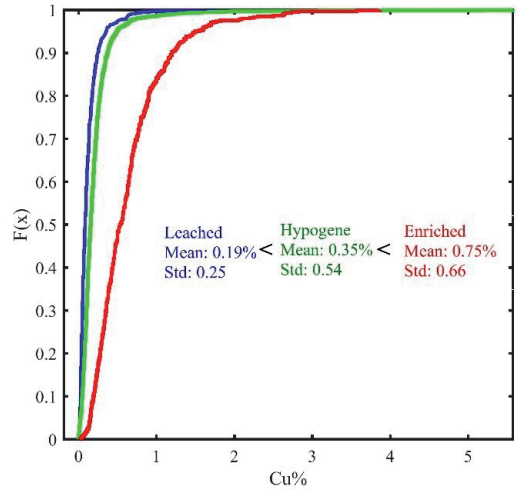

Fig. 4 - Empirical cumulative distribution functions (CDF) and summary statistics of Cu concentration (%) in different mineralisation zones; leached, enriched and hypogene.

Due to the notable thickness of alluvium above the deposit, four zones were considered for simulation: alluvium, leached, enriched, and hypogene (primary sulfide). In mineral exploration activities, drillhole data are usually concentrated in locations with high grades. Therefore, the obtained proportions of the zones do not represent the entire deposit, and drillhole data should initially be declustered. Among different declustering methods, we have used cell declustering in the WinGsilb software package. The whole deposit is divided into cells with specific dimensions. Total occupied cells are counted (n_{oc}) and all cells are given the same weight ($1/n_{oc}$). If there is more than one sample in a cell, they share the weight assigned to the cell (Deutsch, 1989). The weights define the correction for the global proportion. The new proportions (Table 1) were used as the target global proportions for simulation. Next, we computed the transition probability matrix (Table 2), another simulation target, by using a slightly modified version of the method proposed by Pyrcz *et al.* (2008). Thus, data weights derived from cell declustering were used

to calculate the transition probability matrix. Instead of counting the number of transitions from $Z(u)$ to $Z(u + h)$, we considered the mean declustering weights of these two data locations. Applying this approach makes the transition probability matrix a better representation of the vertical inter-relationships of zones.

Table 1 - Proportions of the zones in drillhole data in two cases of raw data and declustered data.

	Alluvium	Leached	Enriched	Hypogene
Raw data	0.139	0.159	0.158	0.544
Declustered data	0.140	0.166	0.135	0.559

Table 2 - Transition probability matrix of drillhole data for lag h (x, y, z) = (0, 0, +1).

	Alluvium	Leached	Enriched	Hypogene
Alluvium		0	0	0
Leached	0.234		0	0
Enriched	0.018	0.301		0
Hypogene	0.026	0.086	0.335	

3.1. TI

Considering the discussed methodology, a TI is constructed based on drillhole data in a small part of the study area. The TI is created manually. First, an initial TI is made and evaluated based on the mentioned criteria. The initial TI is then corrected for second, third and so on times, to achieve a desirable TI.

The global proportions (Table 3) and transition probability matrix (Table 4) of TI are similar to those of the targets (Table 1 and Table 2, respectively). The surface topography information of TI area was imposed on constructed TI. As a result, a TI was generated (Fig. 5) in which the correlation between Z_1 and Z_2 was the same as the corresponding correlation value observed in drillhole data (Fig. 6). In the end, the absolute compatibility of the obtained TI patterns with the data patterns was assessed in different orders of n. The results revealed an acceptable compatibility between TI patterns and drillhole data patterns (Fig. 7).

Table 3 - Global proportions of the zones in constructed TI.

Alluvium	Leached	Enriched	Hypogene
0.14	0.17	0.13	0.56

Table 4 - Transition probability matrix of constructed TI lag h (x, y, z) = (0, 0, +1).

	Alluvium	Leached	Enriched	Hypogene
Alluvium		0	0	0
Leached	0.234		0	0
Enriched	0.016	0.302		0
Hypogene	0.026	0.086	0.336	

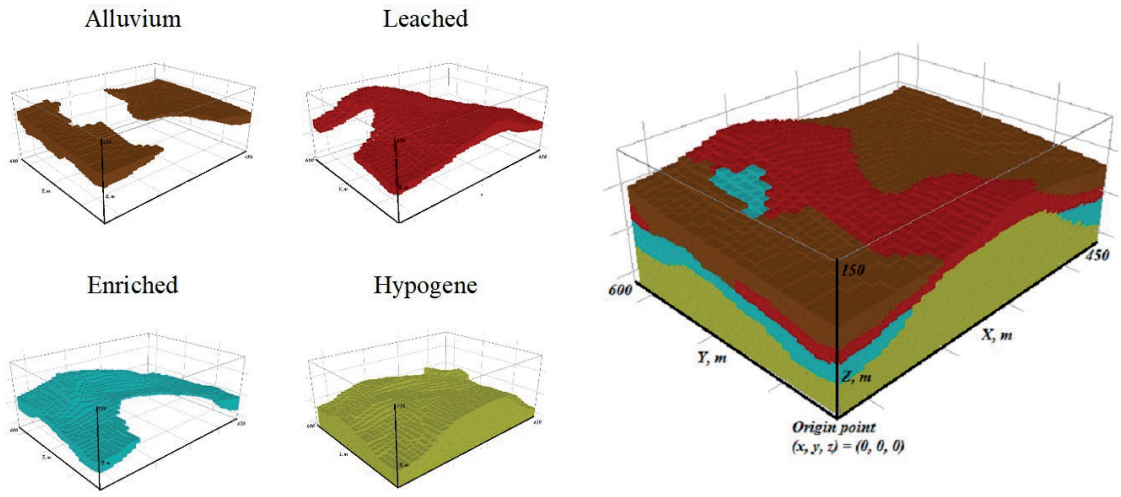

Fig. 5 - 3D view of the constructed TI for the case of Ali-Abad Cu porphyry deposit.

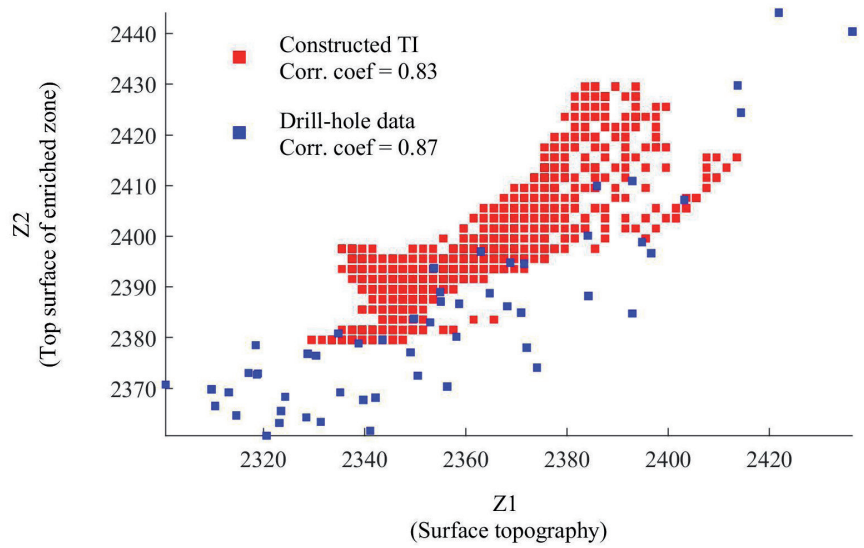

Fig. 6 - The relationship between Z_1 (surface topography) and Z_2 (top surface of the enriched zone) in drillhole data and the constructed TI; this indicates that variations of spatial geometry of contact between zones in TI are the same as what occurs in reality.

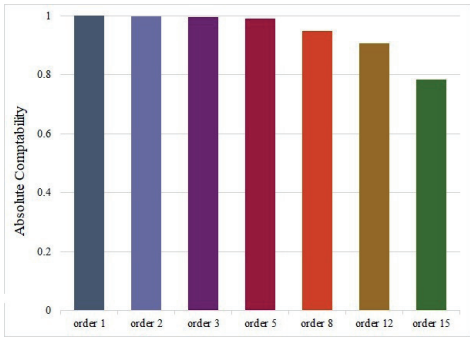

Fig. 7 - Absolute compatibility of the TI patterns with the data patterns was assessed in different orders of neighbours (*n*); this means that the constructed TI is an appropriate representative of realistic spatial patterns extracted from drillhole data.

3.2. SNESIM parameters

Whereas all other input parameters were assigned a constant value, servosystem correction factor λ was assigned different values (0, 0.1, 0.2, …, 1) and SNESIM was used to generate one realisation in each case. For each case, the JSD between transition probabilities and global proportions of a given realisation and those of the targets (Tables 1 and 2) was calculated. Based on the results, λ = 0.8 showed the best reproduction of targets and was accordingly chosen as the best case (Fig. 8). In this case, there is the desired equilibrium between the reproduction of realistic geological patterns and target global proportions.

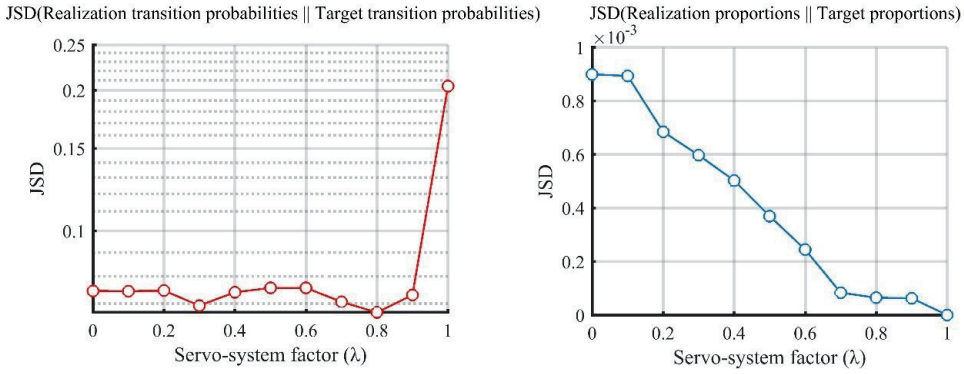

Fig. 8 - The impact of servo-system increase on the reproduction of target proportions (right) and target transition probability matrix (left) of realisations; the case of λ = 0.8 shows the desired equilibrium between the reproduction of realistic geological patterns and target global proportions.

In SNESIM, the search ellipsoid geometry is determined based on its search radius (h_{max}, h_{med}, h_{min}) and the direction of h_{max}. In order to select the direction of h_{max}, we generated a realisation for each of 313 different cases by considering h_{max} = 300 m, h_{med} = 150 m, h_{min} = 50 m, and different combinations of azimuth and dip of h_{max} direction [azimuth = (0, 15, 30, …, 345) and dip = (0, 7.5, 15, …, 90)]. Then, for each case, the JSD between transition probabilities of a given realisation and those of the targets was calculated (Fig. 9). Because it yielded minimum JSD, the zero value was chosen as the best dip value of h_{max}; also, since no azimuth in this dip was superior to others,

h_{max} = h_{med} in a horizontal surface was adopted. Then, to select the best search radiuses, we used the results of the previous step to consider different combinations of h_x = h_y and h_z. One realisation was generated in each case and the JSD between transition probabilities of each realisation and those of the targets was calculated (Fig. 10). Because of h_x = h_y = 150 m and h_z = 50 m resulted in minimum JSD, it was chosen as the best case. It should be noted that if two search ellipsoids with the same JSD have different geometries, the smaller one should be chosen in order to reduce SNESIM computational cost.

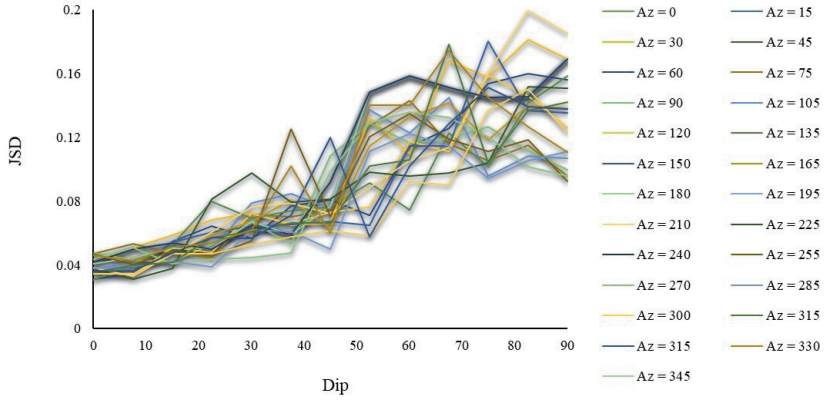

Fig. 9 - The impact of search ellipsoid rotation in different 3D directions on JSD between transition probabilities of realisations and targets. The cases in which dip direction of search ellipsoid is equal to zero, illustrate the best reproduction of target transition probabilities (minimum JSD).

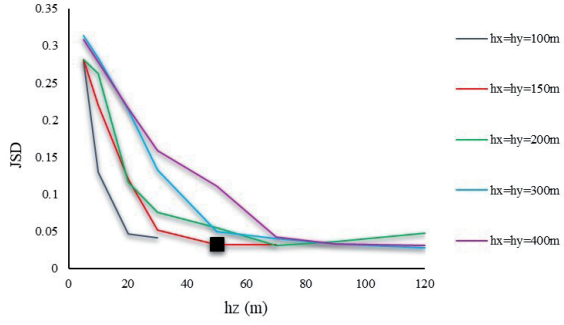

Fig. 10 - The impact of different search ellipsoid radiuses on JSD between realisation transition probabilities of realisations and targets. The black square is related to the case of h_x = h_y = 150 m, h_z = 50 m in which the best reproduction of target transition probabilities was found (minimum JSD).

3.3. VPM

By considering the surface topography as the reference level, we calculated the VPCs between each pair of adjacent drillholes in the E-W and N-S directions. Then, the resulting values were assigned to half of the distance of adjacent drillholes. Next, the values obtained for the proportions of each facies were estimated by the kriging method throughout the simulation grid

where the size of each cell is 10×10×2 m^3. Because the proportions were kriged one by one, they did not reach 1 at each grid node. Therefore, we rescaled the values to ensure that this objective is met. The resulting VPM (Fig. 11) was used as soft probabilities in SNESIM.

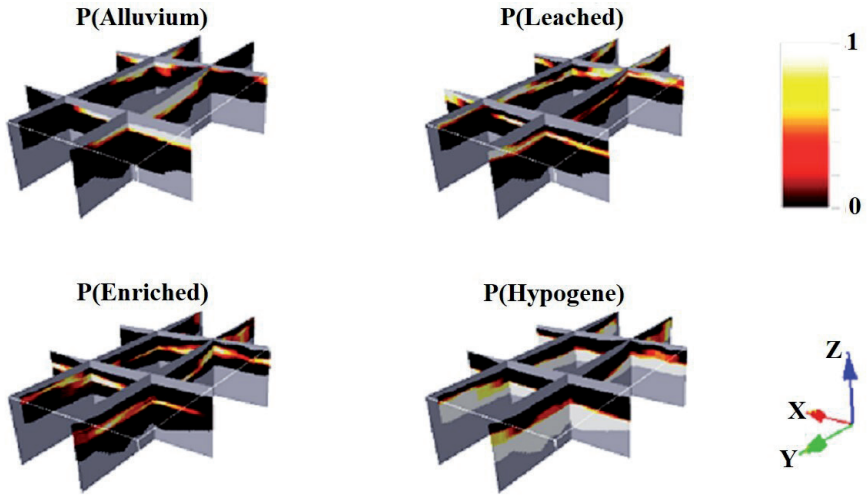

Fig. 11 - The constructed VMP of alluvium, leached, enriched and hypogene zones by analysing the drillhole data set of Ali-Abad Cu porphyry deposit. This VPM was used as soft probabilities in the SNESIM algorithm to address the non-stationarity of local proportions.

3.4. Run SNESIM and validation of the results

Using the constructed TI, hard data, soft probabilities (constructed VPM), defined search ellipsoid, defined servosystem correction factor and other advanced input parameters, 100 realisations were generated. One randomly selected generated realisation is shown in Fig. 12, in which it can clearly be seen that the MPS is capable of reproducing the mineralogical order of the zones.

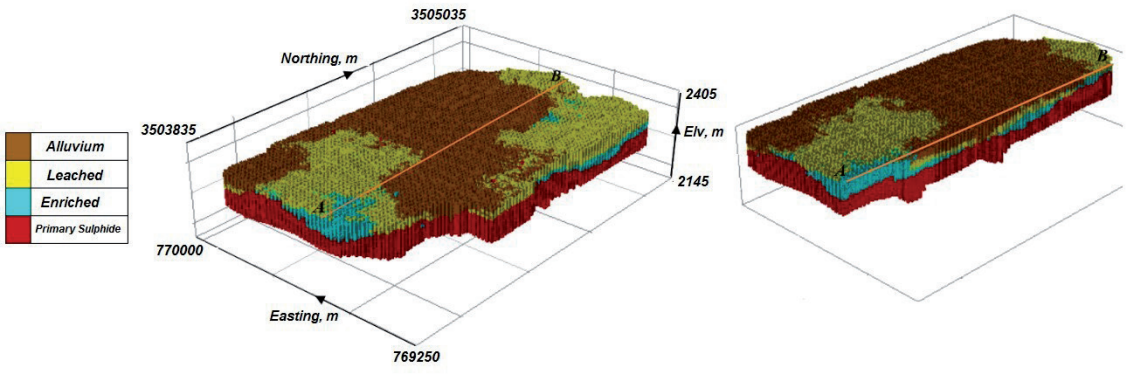

Fig. 12 - The 3D view (left) and cross-sectional view (right) of one randomly selected realisation.

3.5. Validation of the results

We performed the validation procedure of the realisations by using several criteria that are discussed below.

3.5.1. Single-point statistics

Initially, single-point statistics related to the proportions of the zones were compared with target proportions (Fig. 13). The results showed that the difference between the proportion of the zones in different realisations and target proportions is very low. Moreover, using high servo-system correction factor (λ = 0.8) caused stability in reproduction single-point statistics.

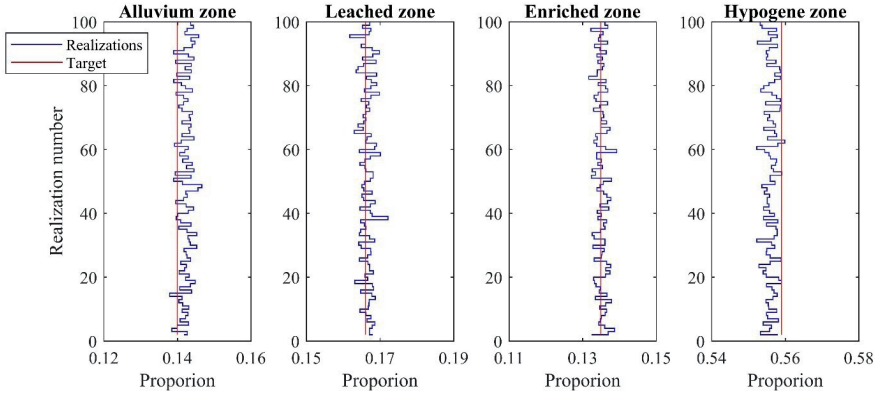

Fig. 13 - Comparison between zones' proportions of SNESIM realisations and target proportions. It can be seen that the zones' proportions were reproduced with high accuracy and precision.

3.5.2. Two-point statistics

Variograms are important tools for measuring the reproduction of two-point statistics. The experimental indicator variograms of leached and enriched zones in the direction of azimuth = 0 and dip = 0 as main spatial continuity direction, were calculated for all realisations and drillhole data (Fig. 14). The results illustrated that the slope and sill values of the variogram of realisations are close to the variogram of drillhole data.

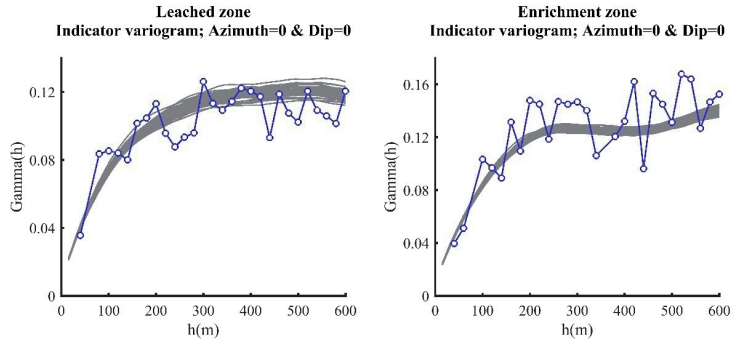

Fig. 14 - The indicator variogram of 100 SNESIM realisations (grey lines) against the indicator variogram of data (blue lines) for leached (left) and enriched (right) zones in the direction of azimuth = 0 and dip = 0; it can be seen that the slope and sill values of the variogram of realisations are close to the variogram of drillhole data.

3.5.3. Transition probabilities

Transition probabilities were calculated over six random realisations and compared with transition probabilities of the targets. The results showed that the SNESIM algorithm is capable of reproducing geologically feasible transitions or desired geological patterns in realisations (top diagrams in Fig. 15). However, transitions with zero targets or geologically impossible transitions, have also been reproduced in realisations with low probability (bottom diagrams in Fig. 15). This unavoidable defect is owing to the attempt of the SNESIM algorithm to simulate both target global proportions and target local proportions.

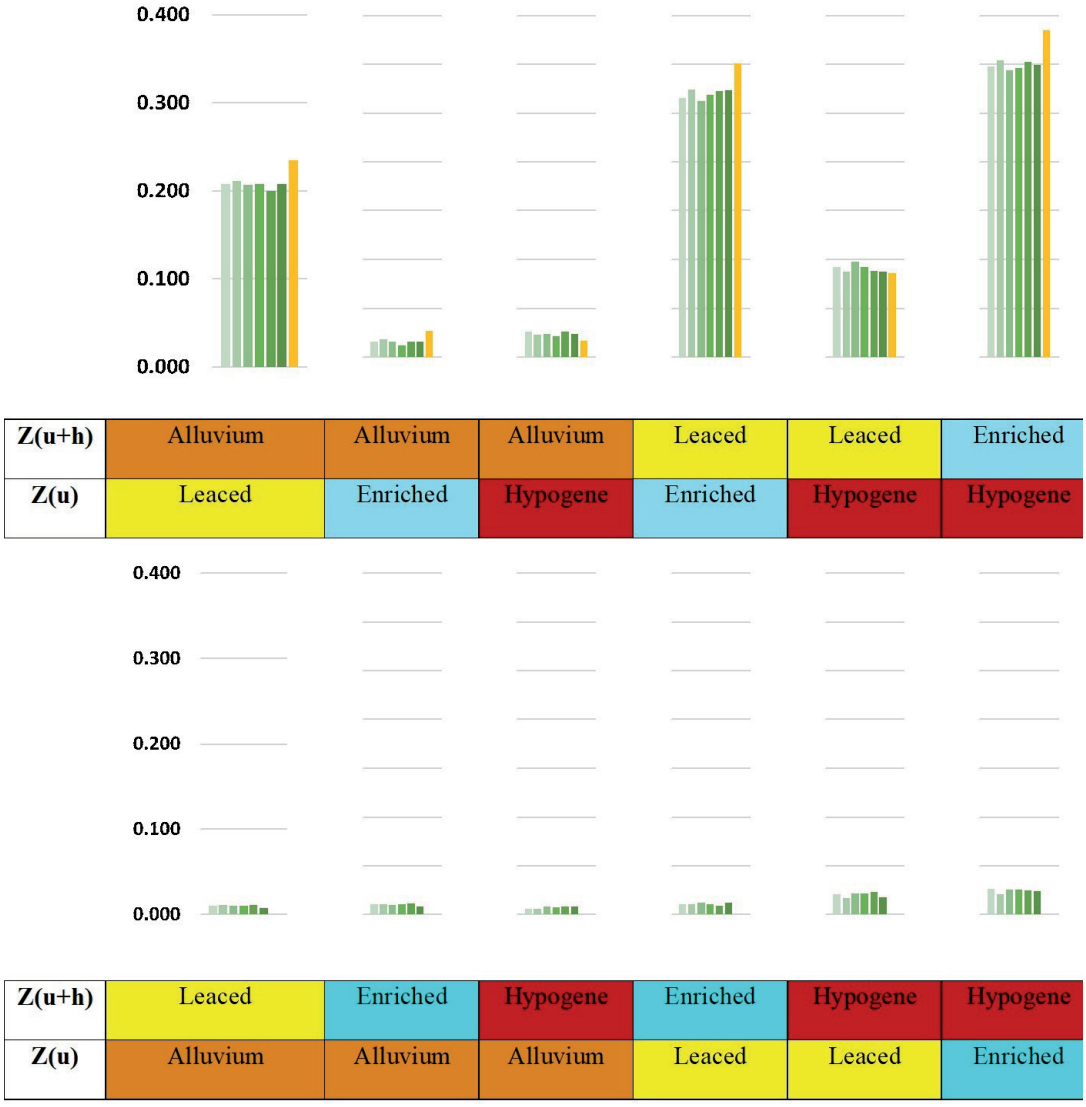

Fig. 15 - Transition probabilities of six randomly selected realisations (green bars) and their comparison with target transition probabilities (yellow bars); transitions that are geologically feasible (top diagrams); and transitions that are not geologically feasible (bottom diagrams).

3.5.4. The impact of using soft probabilities

A total of 100 realisations were generated by the SNESIM algorithm in both cases of using and not using soft probability. The horizontal cross-section of the three randomly selected SNESIM realisations in both of these cases is depicted in Fig. 16. The results suggested that using soft probabilities serves as a guide for SNESIM to control the trends. Additionally, it is evident that SNESIM produces more stable results in the case of using soft probabilities.

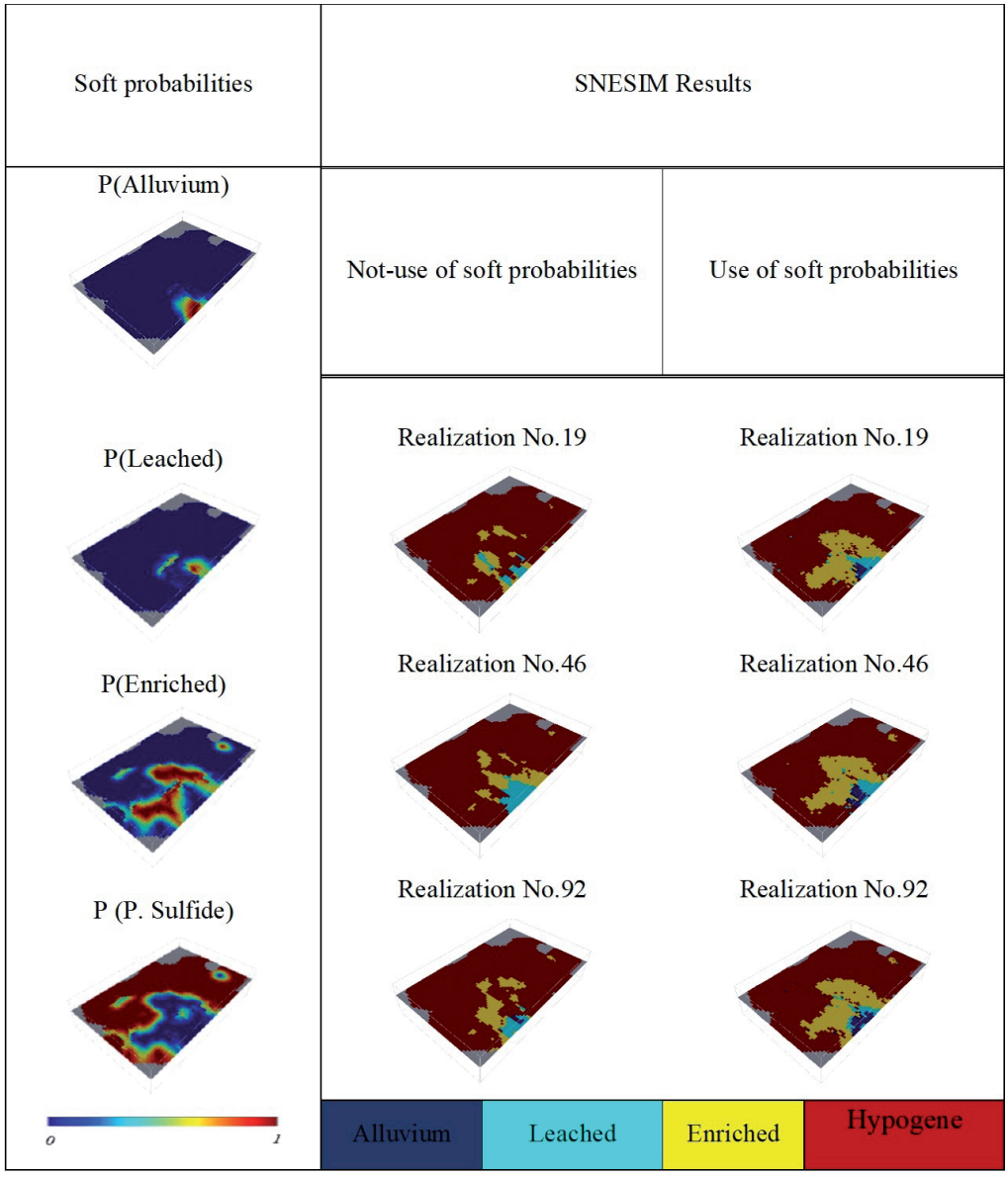

Fig. 16 - Graphical representation of the impact of using soft probabilities on controlling non-stationarity of the zones; using soft probabilities serves as a guide for SNESIM to control the trend of the zones and helps SNESIM produce more stable results.

4. Conclusions

Using the SNESIM algorithm, this study proposed a methodology for building a geological model of mineralisation zones formed by oxidation and enrichment processes in porphyry copper deposits.

The transition probability matrix is a useful tool to quantify the mineralogical order of geological zones. SNESIN, as an MPS method, is capable of simulating the mineralogical order of zones into desired geological patterns. Using this algorithm, we managed to simulate the target proportions with good accuracy and stability in the realisations. This is because of the equivalence of the proportions in the TI with the target proportions and on choosing the best value for the servo-system correction factor. Although selecting or constructing an appropriate TI is the most important and challenging step of an MPS, controlling effective parameters in SNESIM, including the servo-system correction factor and the search ellipsoid, yields more desirable results. Considering soft probabilities in SNESIM helps better control non-stationarity and reduce the entropy of simulation results. However, any attempt by SNESIM to simulate target proportions or involve soft probabilities reduces the reproducibility of desired TI patterns, implying that the input parameters of SNESIM are highly interactive. This interaction must be inferred from a sensitivity analysis and then considered in the simulation process. The methodology followed in this paper could be used to simulate other subsurface geological phenomena in which the vertical mineralogical order is geologically significant.

As observed in this study, a multiple-point geostatistical simulation approach allows geoscience modellers to formulate any geological concepts related to the phenomenon under study in the form of a TI and use it to achieve final models, which are reliable from a geological viewpoint. Given that most of the sufficient geological knowledge of the subsurface phenomenon under study is available, this knowledge can be incorporated in the TI with the opinion of geological experts and, then, acceptable models of geological subsurface phenomena can be achieved.

Acknowledgments. The authors would like to thank the Ali-Abad mining complex for providing the data sets.

REFERENCES

Abdollahifard M.J., Baharvand M. and Mariéthoz G.; 2019: *Efficient training image selection for multiple-point geostatistics via analysis of contours*. Comput. Geosci., 128, 41-50.

Armstrong M., Galli A., Beucher H., Loc'h G., Renard D., Doligez B., Eschard R. and Geffroy F.; 2011: *Plurigaussian simulations in geosciences*, *2nd ed*. Springer Science & Business Media, Dordrecht, The Netherlands, 186 pp.

Arpat G.B. and Caers J.; 2007: *Conditional simulation with patterns*. Math. Geol., 39, 177-203.

Berger B.R., Ayuso R.A., Wynn J.C. and Seal R.R.; 2008: *Preliminary model of porphyry copper deposits*. U.S. Geological Survey, Reston, VA, USA, Open-file report, 1321, 55 pp.

Beucher-Darricau H., Doligez B. and Yarus J.M.; 2006: *Modeling complex reservoirs with multiple conditional techniques: a practical approach to reservoir characterization*. In: Coburn T.C., Yarus M.J. and Chambers R.L. (eds), Stochastic modeling and geostatistics: principles, methods, and case studies, AAPG Computer Applications in Geology, Tulsa, OK, USA, Vol. II, Chapter 5, pp. 289-299.

Boisvert J.B., Pyrcz M.J. and Deutsch C.V.; 2007: *Multiple-point statistics for training image selection*. Nat. Resour. Res., 16, 313-321.

Comunian A., Renard P. and Straubhaar J.; 2012: *3D multiple-point statistics simulation using 2D training images*. Comput. Geosci., 40, 49-65.

Condon L.E. and Maxwell R.M.; 2015: *Evaluating the relationship between topography and groundwater using outputs from a continental-scale integrated hydrology model*. Water Resour. Res., 51, 6602-6621.

Deutsch C.; 1989: *DECLUS*: *a FORTRAN77 program for determining optimum spatial declustering weights*.

Comput. Geosci., 15, 325-332.

Dunham S. and Vann J.; 2007: *Geometallurgy, geostatistics and project value - Does your block model tell you what you need to know?* In: Proc. Project Evaluation 2007, The Australasian Institute of Mining and Metallurgy, Melbourne, Australia, pp. 189-196.

Emery X.; 2007: *Simulation of geological domains using the plurigaussian model: new developments and computer programs*. Comput. Geosci., 33, 1189-1201.

Guardiano F.B. and Srivastava R.M.; 1993: *Multivariate geostatistics: beyond bivariate moments*. In: Soares A. (ed), Geostatistics Troia '92, Quantitative Geology and Geostatistics, Springer, Dordrecht, The Netherlands, Vol. 5, pp. 133-144, doi: 10.1007/978-94-011-1739-5_12.

Hansen T.M., Vu L.T. and Bach T.; 2016: *MPSLIB: a C++ class for sequential simulation of multiple-point statistical models*. SoftwareX, 5, 127-133, doi: 10.1016/J.SOFTX.2016.07.001.

Hosseini S. and Asghari O.; 2016: *Multivariate geostatistical simulation of the Gole Gohar iron ore deposit, Iran*. J. South Afr. Inst. Min. Metall., 116, 423-430.

King F.H.; 1899: *Principals and conditions of the movement of ground water*. U.S. Geological Survey, Washington, DC, USA, 19th Annual Report, part 2, pp. 59-294.

Liu Y.; 2006: *Using the Snesim program for multiple-point statistical simulation*. Comput. Geosci., 32, 1544-1563.

Maharaja A.; 2008: *TiGenerator: object-based training image generator*. Comput. Geosci., 34, 1753-1761.

Mariethoz G. and Caers J.; 2014: *Multiple-point geostatistics: stochastic modeling with training images*. John Wiley & Sons, Hoboken, NJ, USA, 376 pp.

Mariethoz G., Renard P. and Straubhaar J.; 2010: *The direct sampling method to perform multiple-point geostatistical simulations*. Water Resour. Res., 46, W11536, doi: 10.1029/2008WR007621.

Mariethoz G., Straubhaar J., Renard P., Chugunova T. and Biver P.; 2015: *Constraining distance-based multipoint simulations to proportions and trends*. Environ. Modell. Softw., 72, 184-197.

Matheron G., Beucher H., de Fouquet C., Galli A., Guerillot D. and Ravenne C.; 1987: *Conditional simulation of the geometry of fluvio-deltaic reservoirs*. In: Proc. SPE Annual Technical Conference and Exhibition, Dallas, TX, USA, SPE-16753-MS, doi: 10.2118/16753-MS.

Osterholt V. and Dimitrakopoulos R.; 2018: *Simulation of orebody geology with multiple-point geostatistics - Application at Yandi channel iron ore deposit, WA, and implications for resource uncertainty*. In: Dimitrakopoulos R. (ed), Advances in Applied Strategic Mine Planning, Springer, Cham, Switzerland, pp. 335-352, doi: 10.1007/978-3-319-69320-0_22.

Pérez C., Mariethoz G. and Ortiz J.M.; 2014: *Verifying the high-order consistency of training images with data for multiple-point geostatistics*. Comput. Geosci., 70, 190-205.

Pyrcz M.J., Boisvert J.B. and Deutsch C.V.; 2008: *A library of training images for fluvial and deepwater reservoirs and associated code*. Comput. Geosci., 34, 542-560.

Ravenne C., Galli A., Doligez B., Beucher H. and Eschard R.; 2002: *Quantification of facies relationships via proportion curves*. In: Armstrong M., Bettini C., Champigny N., Galli A. and Remacre A. (eds), Geostatistics Rio 2000, Quantitative Geology and Geostatistics, Springer, Dordrecht, The Netherlands, vol. 12, pp. 19-39, doi: 10.1007/978-94-017-1701-4_3.

Rezaee H. and Marcotte D.; 2017: *Integration of multiple soft data sets in MPS thru multinomial logistic regression: a case study of gas hydrates*. Stochastic Environ. Res. Risk Assess., 31, 1727-1745.

Rezaee H., Mariethoz G., Koneshloo M. and Asghari O.; 2013: *Multiple-point geostatistical simulation using the bunch-pasting direct sampling method*. Comput. Geosci., 54, 293-308.

Rezaee H., Asghari O., Koneshloo M. and Ortiz J.M.; 2014: *Multiple-point geostatistical simulation of dykes: application at Sungun porphyry copper system, Iran.* Stochastic Environ. Res. Risk Assess., 28, 1913-1927.

Sillitoe R.H.; 2005: *Supergene oxidation and enrichment porphyry copper and related deposits*. Econ. Geol., 100, 723-768.

Straubhaar J., Walgenwitz A. and Renard P.; 2013: *Parallel multiple-point statistics algorithm based on list and tree structures*. Math. Geosci., 45, 131-147.

Strebelle S.; 2002: *Conditional simulation of complex geological structures using multiple-point statistics*. Math. Geol., 34, 1-21.

Tahmasebi P.; 2018: *Multiple point statistics: a review*. In: Daya Sagar B., Cheng Q. and Agterberg F. (eds), Handbook of Mathematical Geosciences, Springer, Cham, Switzerland, pp. 613-643, doi: 10.1007/978-3-

319-78999-6_30.

Talebi H., Asghari O. and Emery X.; 2013: *Application of plurigaussian simulation to delineate the layout of alteration domains in Sungun copper deposit*. Cent. Eur. J. Geosci., 5, 514-522.

Talebi H., Asghari O. and Emery X.; 2014: *Simulation of the lately injected dykes in an Iranian porphyry copper deposit using the plurigaussian model*. Arabian J. Geosci., 7, 2771-2780.

Talebi H., Asghari O. and Emery X.; 2015: *Stochastic rock type modeling in a porphyry copper deposit and its application to copper grade evaluation*. J. Geochem. Explor., 157, 162-168.

Talesh Hosseini S., Asghari O., Torabi S.A. and Abedi M.; 2020: *An optimum selection of simulated geological models by multi-point geostatistics and multi-criteria decision-making approaches*; *a case study in Sungun porphyry-Cu deposit, Iran.* J. Min. Environ., 11, 481-503.

Tehrani M.M., Asghari O. and Emery X.; 2013: *Simulation of mineral grades and classification of mineral resources by using hard and soft conditioning data*: *application to Sungun porphyry copper deposit.* Arabian J. Geosci., 6, 3773-3781.

Tran T.T.; 1994: *Improving variogram reproduction on dense simulation grids*. Comput. Geosci., 20, 1161-1168.

Zarasvandi A., Liaghat S. and Zentilli M.; 2005: *Geology of the Darreh-Zerreshk and Ali-Abad porphyry copper deposits, central Iran.* Int. Geol. Rev., 47, 620-646.

Zhang T., Switzer P. and Journel A.; 2006: *Filter-based classification of training image patterns for spatial simulation*. Math Geol., 38, 63–80.

Corresponding author: Omid Asghari
Simulation and Data Processing Laboratory, University College of Engineering, School of Mining Engineering, University of Tehran
North Kargar, Tehran, Iran
Phone: + 39 21 82084229; e-mail: o.asghari@ut.ac.ir